

Quantum Magnetic Excitations from Stripes in Cuprate Superconductors

J. M. Tranquada¹, H. Woo^{1,2}, T. G. Perring², H. Goka³, G. D. Gu¹, G. Xu¹, M. Fujita³, and K. Yamada³

¹*Physics Department, Brookhaven National Laboratory, Upton, NY 11973, USA*

²*ISIS Facility, Rutherford Appleton Laboratory, Chilton, Didcot, Oxon OX11 0QX, UK*

³*Institute for Materials Research, Tohoku University, Sendai, 980-8577, Japan*

The nature of the antiferromagnetic spin excitations in copper-oxide superconductors,¹ generally believed² to play a significant role in the pairing mechanism, remains a matter of controversy. One school of thought holds that they are associated with the response of low-energy charge carriers close to the Fermi energy.³ In an alternative approach, the spin fluctuations are due to remnants of the antiferromagnetic-insulator phase that is obtained when the charge carriers are removed; spatial segregation of the carriers into inhomogeneous patterns, such as stripes, allow the antiferromagnetic regions to survive.⁴ Recently, it has been argued that measurements of the dispersion of spin excitations in superconducting $\text{YBa}_2\text{Cu}_3\text{O}_{6+x}$ are incompatible with the latter picture.⁵ Here we present a neutron-scattering study of magnetic fluctuations in a particular cuprate, $\text{La}_{1.875}\text{Ba}_{0.125}\text{CuO}_4$, that exhibits inhomogeneous, charge-stripe order.⁶ We show that 1) the high-energy excitations are distinct from spin waves and similar to those of quantum spin structures, such as two-leg ladders, and 2) dispersion features similar to those in $\text{YBa}_2\text{Cu}_3\text{O}_{6+x}$ are present. This implies that the important magnetic correlations in the cuprates universally result from charge inhomogeneity.

$\text{La}_{2-x}\text{Ba}_x\text{CuO}_4$ ("Zurich" oxide) is the material in which Bednorz and Müller¹ first discovered high-temperature superconductivity. Not long after that, an anomalous suppression of the superconductivity in a very narrow region about $x = 1/8$ was found by Moodenbaugh *et al.*⁷ That anomaly was later shown to be associated with charge and spin stripe order.⁸ Schematic diagrams of stripe order in the CuO_2 planes are shown in Fig. 1(a) and (b). Between the charge stripes are regions with locally-antiferromagnetic order. While the specific alignment of the stripes with respect to the lattice and the effective widths of the magnetic domains have not been directly determined by experiment, the configuration shown (commonly called "bond-centered" stripes) has received particular theoretical attention.⁹⁻¹³

In a uniform, two-dimensional, antiferromagnetic CuO_2 plane, with lattice parameter $a = 3.8 \text{ \AA}$ between the nearest-neighbor Cu ions, a neutron diffraction measurement yields superlattice peaks characterized by the wave vector $\mathbf{Q}_{\text{AF}} = (1/2, 1/2)$, in units of $2\pi/a$. When vertical stripe order is present, the superlattice peaks move to $(1/2 \pm \delta, 1/2)$, where $\delta = 1/(2p)$, and p is the charge stripe spacing; $p = 4$ in the present case. Analogous peaks appear for the case of horizontal stripes [see Fig. 1(f),(g)]. In $\text{La}_{1.875}\text{Ba}_{0.125}\text{CuO}_4$, both stripe orientations are present, so one observes both sets of superlattice peaks simultaneously [see Fig. 1(i)].

The ordered magnetic moments can fluctuate about their average orientations. It costs energy to create these fluctuations, and the variation of the magnetic excitation energy with wave vector \mathbf{Q} can be measured with inelastic neutron scattering. Antiferromagnetic La_2CuO_4 exhibits conventional spin-wave behavior,^{14,15} with an energy dispersion $\hbar\omega = c|\mathbf{Q} - \mathbf{Q}_{\text{AF}}|$ for $\hbar\omega < J$, with J being the effective superexchange coupling between neighboring magnetic moments. The spin-wave velocity c is proportional to J , and the spin waves extend up to a maximum energy of $2J$. The strength of the magnetic scattering is relatively large throughout the antiferromagnetic

Brillouin zone centered on \mathbf{Q}_{AF} [indicated by the dashed-line diamond in Fig. 1(f),(g),(i)], but becomes negligible outside of that zone.

One might expect to find spin waves dispersing out of the superlattice peaks of $\text{La}_{1.875}\text{Ba}_{0.125}\text{CuO}_4$,¹⁶⁻¹⁸ in the form of expanding cones as shown in Fig. 1(d). The dispersion of spin waves has recently been measured in the stripe-ordered model compound $\text{La}_{2-x}\text{Sr}_x\text{NiO}_4$,^{19,20} where $S = 1/2$ Cu spins are replaced by $S = 1$ Ni spins and the stripes run diagonally. In $\text{La}_{1.875}\text{Ba}_{0.125}\text{CuO}_4$ and a related compound,²¹ the low-energy excitations (< 12 meV) appear similar to spin waves with a large velocity c .

Given the robust nature of superconductivity in the layered cuprates, one expects there to be more or less universal behavior of important features such as the magnetic-excitation spectra. The problem with the spin-wave picture for $\text{La}_{1.875}\text{Ba}_{0.125}\text{CuO}_4$, then, is that it would be inconsistent with the spectrum measured in superconducting $\text{YBa}_2\text{Cu}_3\text{O}_{6+x}$.⁵ For samples of the latter material with a superconducting transition temperature, T_c , of ~ 90 K, a prominent peak in the magnetic scattering is found at ~ 40 meV centered on \mathbf{Q}_{AF} when $T < T_c$. Below this energy, the magnetic excitations disperse downwards [see Fig. 4(d)].

There are at least two possibilities for the higher-energy magnetic-excitation spectrum in $\text{La}_{1.875}\text{Ba}_{0.125}\text{CuO}_4$: 1) it is spin-wave like, indicating that the stripe-ordered material is quite different from a good superconducting sample, or 2) it is similar to $\text{YBa}_2\text{Cu}_3\text{O}_{6+x}$ and different from the spin-wave form, for reasons yet to be understood. To settle this question, we have grown large, high-quality crystals of $\text{La}_{1.875}\text{Ba}_{0.125}\text{CuO}_4$ and studied them with a powerful time-of-flight neutron spectrometer, MAPS, at the ISIS spallation source.

To present the experimental results, we find it convenient to change to a coordinate system rotated by 45° [see Fig. 1(k),(l)], in which $\mathbf{Q}'_{\text{AF}} = (1,0,0)$ [measured in units of $2\pi/(\alpha\sqrt{2})$]. (We will use ' to indicate wave vectors in the rotated system.) In this rotated system, the antiferromagnetic zone becomes a square box, on which we will focus.

Experimental measurements are presented in Fig. 2. These are constant-energy slices through the magnetic scattering, with the energy transfer, $E = \hbar\omega$, increasing from the lower left to upper right. The magnetic scattering is centered on \mathbf{Q}'_{AF} ; there are also features due to phonons, and "background" from single- and multiple-phonon scattering. At 6 meV, one can clearly see the four incommensurate peaks, corresponding to fluctuations about the ordered stripe state. These low-energy results are similar to what is observed in superconducting $\text{La}_{2-x}\text{Sr}_x\text{CuO}_4$.²² By 36 meV, the signal has dispersed inwards towards \mathbf{Q}'_{AF} , nearly forming a ring about that point. A simple commensurate peak is found at 55 meV.

Using a spin-wave model, we would expect the 36-meV data to look something like Fig. 3(a): four rings centered on the incommensurate wave vectors, representing cuts through the spin-wave dispersion cones. This picture is clearly quite different from the experimental results. The behavior at higher energies is even more striking. At 105 meV, the excitations have started to disperse outwards, but note the new shape: it is roughly a diamond, with points rotated 45° from the incommensurate wave vectors. This diamond continues to grow at 160 and 200 meV.

The measured dispersion along $\mathbf{Q}' = (1+q, q, 0)$ is presented in Fig. 4(b). The low-energy dispersion into $q = 0$ near 50 meV is rather similar to that reported in superconducting $\text{YBa}_2\text{Cu}_3\text{O}_{6.85}$,⁵ reproduced in Fig. 4(d). Another interesting quantity to compare is the function $S(\omega)$, obtained by integrating the magnetic scattering

intensity $S(\mathbf{Q}, \omega)$ over \mathbf{Q} . (To obtain just the spin-dependent behavior, we have corrected for the anisotropic magnetic form factor.²³) The results are shown in Fig. 4(a). With increasing energy, $S(\omega)$ initially decreases, and then rises to a broad peak near 50–60 meV. Above that, $S(\omega)$ gradually decreases. These results are qualitatively similar to earlier results on $\text{La}_{2-x}\text{Sr}_x\text{CuO}_4$.²⁴ A model function used to describe measurements²⁵ on $\text{YBa}_2\text{Cu}_3\text{O}_{6.95}$ is shown in Fig. 4(c). (Note that the latter result is for $T \ll T_c$, while ours is for $T > T_c$.) The general features of a peak in $S(\omega)$ in the vicinity of the commensurate scattering, with a substantial decrease at lower energies, are found in both; the main difference is the strength of the incommensurate scattering at low energies for our stripe-ordered sample.

Is there a simple way to understand our observations? If we ignore the low-energy incommensurate scattering, the finite-energy peak in $S(\omega)$ suggests that we are measuring singlet-triplet excitations of decoupled spin clusters. An obvious candidate for such a cluster would be one of the magnetic domains shown in Fig. 1(a) and (b), corresponding to what is commonly called a 2-leg spin ladder [Fig. 1(c)]. (This name refers to the pattern formed by the exchange paths between the magnetic ions.) Now, a spin ladder has rather interesting properties.²⁶ The superexchange between neighboring spins keeps them antiparallel, but there is no static order at any temperature. This fluctuating, correlated state is said to be quantum disordered. There is a substantial energy gap to the first excited state, and the excitations disperse only along the ladder direction, not along the rungs [see Fig. 1(e)].

For a horizontal spin ladder, Fig. 1(c),(e), the minimum spin gap appears along $\mathbf{Q} = (1/2, k)$, for all k , and the maximum energy is reached along $\mathbf{Q}_m = (1/2 \pm 1/4, k)$.²⁷ Because of the singlet correlations, the magnetic scattering is relatively strong for \mathbf{Q} between the lines \mathbf{Q}_m , but weak outside of them. Thus, we may take these lines as defining a magnetic intensity zone. Averaging over both horizontal and vertical ladders,

the intensity zone in our rotated coordinate system forms a diamond within the antiferromagnetic zone [see Fig. 1(n)].

To compare with experiment, we have calculated simulated spectra using the single-mode approximation for the scattering function of a spin ladder with isotropic exchange (Konik and Essler, unpublished)

$$S(\mathbf{Q}, \omega) \sim (\hbar \omega_{q\parallel})^{-1} [\sin^2(q_{\parallel} a/2) + \sin^2(q_{\perp} a/2)] [\delta(\omega - \omega_{q\parallel}) - \delta(\omega + \omega_{q\parallel})].$$

Here, q_{\parallel} is measured parallel to the ladder, q_{\perp} is along the rungs, and the dispersion $\omega_{q\parallel}$ is given by Barnes and Riera²⁷ [see Fig. 1(e)]. Parts of this scattering function have been tested in measurements of ladder excitations on $\text{Sr}_{14}\text{Cu}_{24}\text{O}_{41}$.²⁸ For the simulations in Fig. 3 (b)-(e), the δ -functions are replaced by Lorentzians with energy width Γ . We see that the most intense signal has a diamond shape that disperses outward with energy, similar to the right-hand side of Fig. 2. The calculated and measured $S(\omega)$ and $\omega(q)$ are compared in Fig. 4 (a) and (b), respectively. Reasonable agreement is found.

The low-energy incommensurate scattering can be modelled by allowing weak coupling between the ladders, through the charge stripes. Simulations by Konik and Essler (unpublished) give a quite reasonable fit to the observed dispersion. Furthermore, there are experimental precedents for combined quantum magnetic excitations and low-energy spin waves in systems of weakly-coupled $S = 1$ chains.^{29,30}

In conclusion, we have shown that the magnetic excitations of a stripe-ordered cuprate have a quantum nature at high energies, though they are spin-wave like at the lowest energies. The similarity with reported dispersions for $\text{YBa}_2\text{Cu}_3\text{O}_{6+x}$ strongly suggests that the magnetic correlations relevant to superconductivity in the cuprates are universally associated with quantum structures defined by charge inhomogeneity.

Methods

Four crystals, with a total mass of 58 g, were grown by the travelling-solvent floating-zone method at Brookhaven. Magnetic susceptibility measurements on pieces cut from the ends of each crystal show that T_c is generally less than 3 K, but at one end of each of two crystals it is close to 6 K. The crystal quality was first checked on the BT-9 spectrometer at the NIST Center for Neutron Research, while the mounting and alignment were performed on the KSD spectrometer at the JRR-3M reactor in Tokai, Japan. For the experiment at the MAPS spectrometer, the co-aligned crystals were oriented with their c -axes parallel to the incident beam. In distinguishing the magnetic scattering from other signals, strong contributions from phonon branches at 20 and 47 meV were treated with care.

Received 27 January 2004.

1. Bednorz, J. G., & Müller, K. A. Possible High T_c Superconductivity in the Ba-La-Cu-O System. *Z. Phys. B* **64**, 189-193 (1986).
2. Orenstein, J. & Millis, A. J. Advances in the Physics of High-Temperature Superconductivity. *Science* **288**, 468-474 (2000).
3. Si, Q., Zha, Y., Levin, K., & Lu, J. P. Comparison of spin dynamics in $\text{YBa}_2\text{Cu}_3\text{O}_{7-\delta}$ and $\text{La}_{2-x}\text{Sr}_x\text{CuO}_4$: Effects of Fermi-surface geometry. *Phys. Rev. B* **47**, 9055-9076 (1993).
4. Kivelson, S. A. *et al.* How to detect fluctuating stripes in the high-temperature superconductors. *Rev. Mod. Phys.* **75**, 1201 (2003).

5. Bourges, P. *et al.* The Spin Excitation Spectrum in Superconducting $\text{YBa}_2\text{Cu}_3\text{O}_{6.85}$. *Science* **288**, 1234-1237 (2000).
6. Fujita, M. *et al.* Thermal melting of stripe order in $\text{La}_{1.875}\text{Ba}_{0.125}\text{CuO}_4$ and $\text{La}_{1.875}\text{Ba}_{0.075}\text{Sr}_{0.050}\text{CuO}_4$. *To be published*.
7. Moodenbaugh, A. R. *et al.* Superconducting properties of $\text{La}_{2-x}\text{Ba}_x\text{CuO}_4$. *Phys. Rev. B* **38**, 4596-4600 (1988).
8. Tranquada, J. M. *et al.* Evidence for stripe correlations of spins and holes in copper oxide superconductors. *Nature* **375**, 561-564 (1995).
9. Arrigoni, E., Fradkin, E., & Kivelson, S. A. Mechanism of High Temperature Superconductivity in a Striped Hubbard Model. <http://xxx.arxiv.org/pdf/cond-mat/0309572>.
10. White, S. R. & Scalapino, D. J. Density Matrix Renormalization Group Study of the Striped Phase in the 2D t - J Model. *Phys. Rev. Lett.* **80**, 1272-1275 (1998).
11. Sachdev, S. & Read, N. Large N expansion for frustrated and doped quantum antiferromagnets. *Int. J. Mod. Phys. B* **5**, 219-249 (1991).
12. Zaanen, J. *et al.* The geometric order of stripes and Luttinger liquids. *Phil. Mag. B* **81**, 1485-1531 (2001).
13. Eder, R. & Ohta, Y. Dynamical domain walls and spin-Peierls order in doped antiferromagnets: Evidence from exact diagonalization of small clusters. <http://xxx.arxiv.org/pdf/cond-mat/0304554>.
14. Coldea, R. *et al.* Spin Waves and Electronic Interactions in La_2CuO_4 . *Phys. Rev. Lett.* **86**, 5377-5380 (2001).
15. Kastner, M. A., Birgeneau, R. J., Shirane, G., & Endoh, Y. Magnetic, transport, and optical properties of monolayer copper oxides. *Rev. Mod. Phys.* **70**, 897-928 (1998).

16. Batista, C. D., Ortiz, G., & Balatsky, A. V. Unified description of the resonance peak and incommensuration in high- T_c superconductors. *Phys. Rev. B* **64**, 172508 (2001).
17. Krüger, F. & Scheidl, S. Spin dynamics of stripes. *Phys. Rev. B* **67**, 134512 (2003).
18. Carlson, E. W., Yao, D. X., & Campbell, D. K. Spin wave spectra in the presence of antiphase domain walls. *To be published*.
19. Bourges, P. *et al.* High-Energy Spin Dynamics in $\text{La}_{1.69}\text{Sr}_{0.31}\text{NiO}_4$. *Phys. Rev. Lett.* **90**, 147202 (2003).
20. Boothroyd, A. T. *et al.* Spin dynamics in stripe-ordered $\text{La}_{5/3}\text{Sr}_{1/3}\text{NiO}_4$. *Phys. Rev. B* **67**, 100407 (2003).
21. Ito, M. *et al.* Effects of "stripes" on the magnetic excitation spectra of $\text{La}_{1.48}\text{Nd}_{0.4}\text{Sr}_{0.12}\text{CuO}_4$. *J. Phys. Soc. Jpn.* **72**, 1627-1630 (2003).
22. Cheong, S.-W. *et al.* Incommensurate magnetic fluctuations in $\text{La}_{2-x}\text{Sr}_x\text{CuO}_4$. *Phys. Rev. Lett.* **67**, 1791-1794 (1991).
23. Shamoto, S. *et al.* Neutron-scattering study of antiferromagnetism in $\text{YBa}_2\text{Cu}_3\text{O}_{6.15}$. *Phys. Rev. B* **48**, 13817-13825 (1993).
24. Hayden, S. M. *et al.* Comparison of the High-Frequency Magnetic Fluctuations in Insulating and Superconducting $\text{La}_{2-x}\text{Sr}_x\text{CuO}_4$. *Phys. Rev. Lett.* **76**, 1344-1347 (1996).
25. Reznik, D. *et al.* Dispersion of Magnetic Excitations in Superconducting Optimally Doped $\text{YBa}_2\text{Cu}_3\text{O}_{6.95}$. <http://xxx.arxiv.org/pdf/cond-mat/0307591>.
26. Dagotto, E. & Rice, T. M. Surprises on the Way from One- to Two-Dimensional Quantum Magnets: The Ladder Materials. *Science* **271**, 618-623 (1996).
27. Barnes, T. & Riera, J. Susceptibility and excitation spectrum of $(\text{VO})_2\text{P}_2\text{O}_7$ in ladder and dimer-chain models. *Phys. Rev. B* **50**, 6817-6822 (1994).

28. Eccleston, R. S. *et al.* Spin Dynamics of the Spin-Ladder Dimer-Chain Material $\text{Sr}_{14}\text{Cu}_{24}\text{O}_{41}$. *Phys. Rev. Lett.* **81**, 1702-1705 (1998).
29. Yokoo, T. *et al.* Magnetic ordering, spin waves, and Haldane-gap excitations in $(\text{Nd}_x\text{Y}_{1-x})_2\text{BaNiO}_5$ linear-chain mixed-spin antiferromagnets. *Phys. Rev. B* **58**, 14424-14435 (1998).
30. Xu, G. *et al.* Holes in a Quantum Spin Liquid. *Science* **289**, 419-422 (2000).

Acknowledgements JMT, HW, GDG and GX are supported by the Office of Science, U.S. Department of Energy. KY and MF are supported by the Japanese Ministry of Education, Culture, Sports, Science and Technology. Work supported in part by the U.S.-Japan Cooperative Research Program on Neutron Scattering. We gratefully acknowledge assistance with sample characterization from A. R. Moodenbaugh and Qiang Li, and helpful discussions with E. Carlson, F. Essler, S. A. Kivelson, R. Konik, S. Sachdev, and I. Zaliznyak.

Competing interests statement The authors declare that they have no competing financial interests.

Correspondence and requests for materials should be addressed to JMT (e-mail: jtran@bnl.gov).

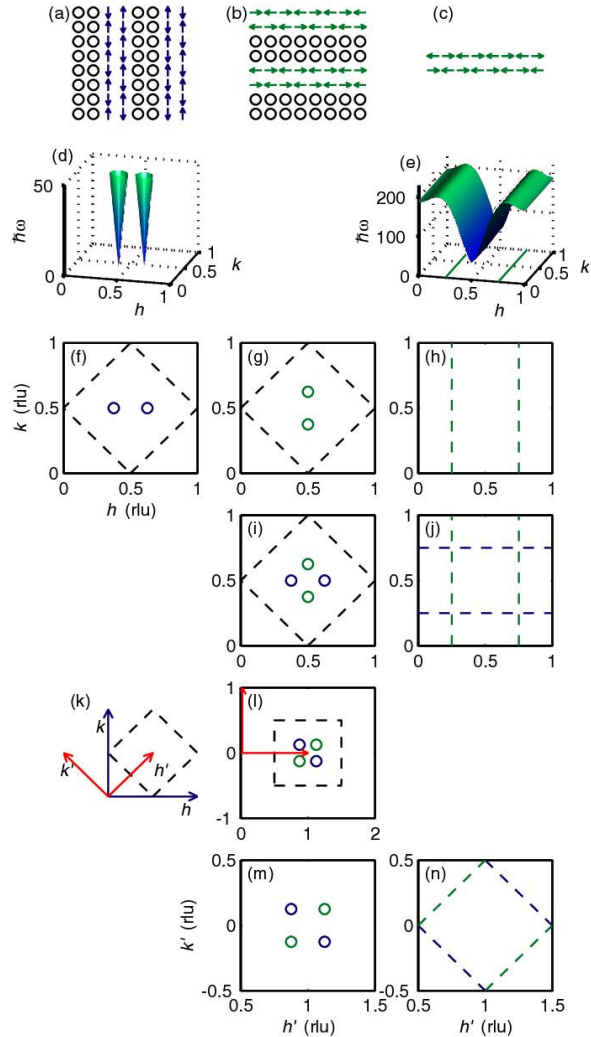


Figure 1 Real-space diagrams of (a) vertical stripes; (b) horizontal stripes; (c) a horizontal spin ladder. Dispersion of (d) spin-waves due to vertical stripes; (e) triplet excitations in a horizontal spin ladder. Reciprocal space, with h and k in reciprocal lattice units (rlu), showing (f) incommensurate magnetic wave vectors for vertical stripe order (dashed line gives antiferromagnetic zone boundary); (g) same for horizontal stripes; (h) intensity zone boundary for a horizontal spin ladder. Wave vectors and boundaries expected when both types of (i) stripes and (j) ladders are present simultaneously. (k) Rotation by 45° to a more convenient coordinate system; (l) incommensurate points in the rotated zone. (m) Expanded view of a single AF zone in the rotated zone; (n) same showing the "zone boundaries" for ladders.

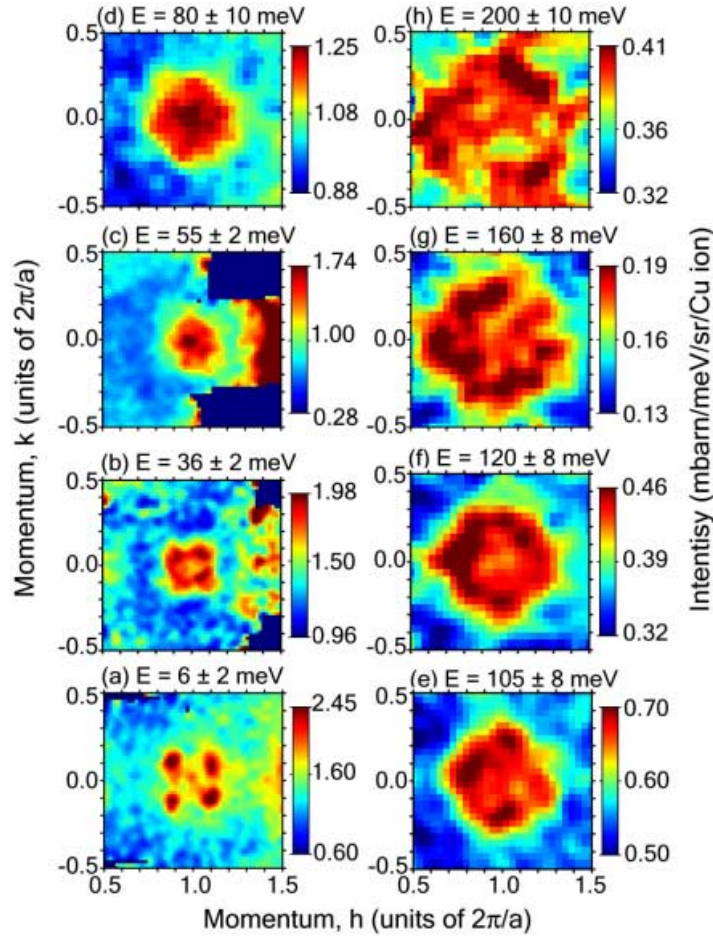


Figure 2 Experimental results: constant-energy slices through the magnetic scattering of $\text{La}_{1.875}\text{Ba}_{0.125}\text{CuO}_4$ measured at 12 K ($> T_c$). Intensity is plotted in false color within a single antiferromagnetic zone [c.f. Fig. 1(m),(n)]. Energy has been integrated over the ranges indicated by the error bars, and \mathbf{Q} dependence has been convolved with a Gaussian to reduce scatter. Panels (a)-(c) measured with an incident neutron energy $E_i = 80$ meV, (d) and (e) with $E_i = 240$ meV, and (f) with $E_i = 500$ meV.

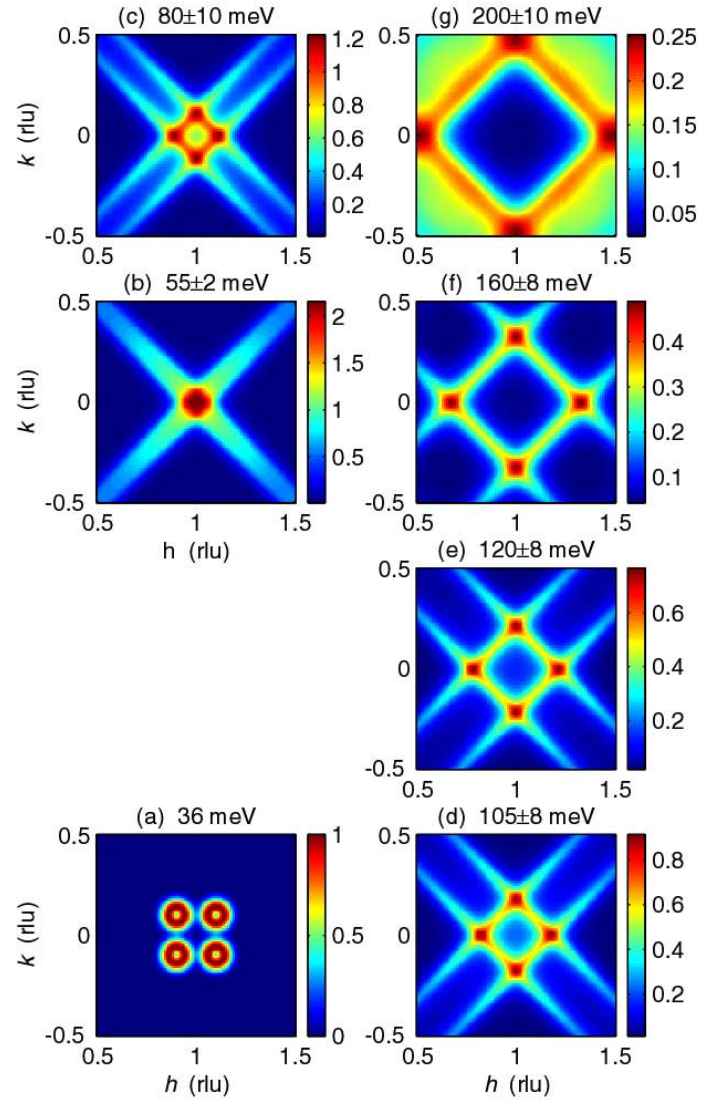


Figure 3 Simulations of constant-energy slices. (a) Spin-wave model for $\hbar\omega = 36$ meV. (b)-(g) 2-leg ladder model, using $J = 100$ meV and $\Gamma/J = 0.2$. In all cases, we have averaged over both orientations (horizontal and vertical) of stripes or spin ladders, and have integrated over the same energy ranges as in Fig. 2.

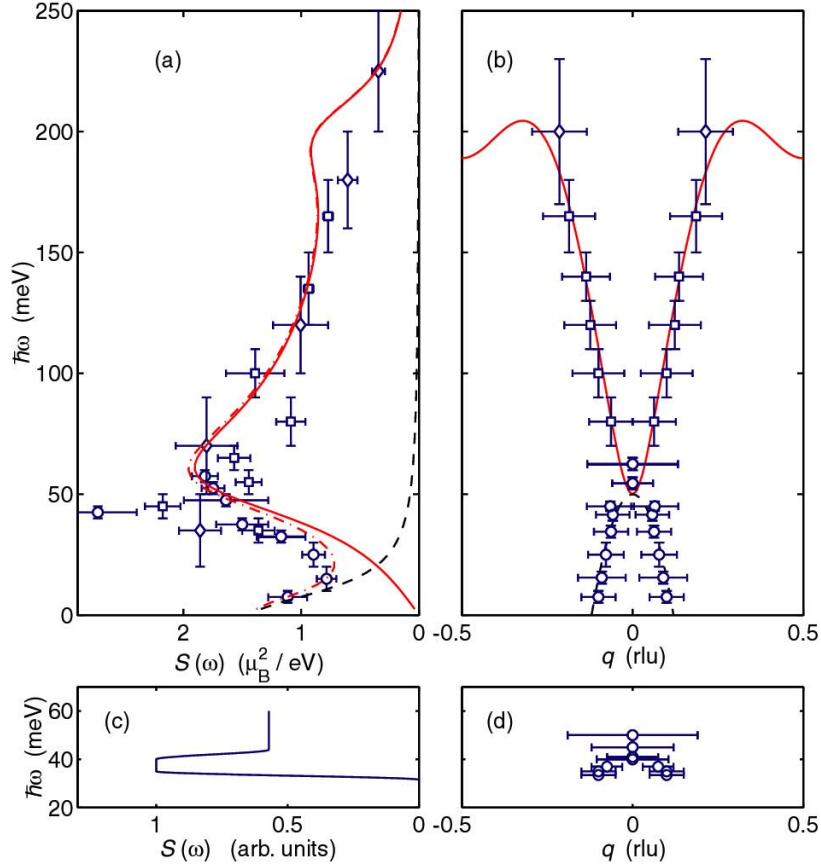


Figure 4 (a) $S(\omega)$, as defined in the text. Circles: $E_i = 80$ meV data set; squares: $E_i = 240$ meV; diamonds: $E_i = 500$ meV. (b) Dispersion measured along $\mathbf{Q}' = (1+q, q)$, with the assumption of symmetry about $q = 0$. Red lines in (a) and (b) are calculated from the 2-leg spin ladder model with the same parameters as in Fig. 3. Black dashed line in (a) is a Lorentzian to describe the low energy signal, and the red dot-dashed line is the sum of the other two curves. Vertical "error" bars in (a) and (b) indicate the energy range over which data were integrated, while horizontal bars in (b) indicate the q width of the signal. (c) $S(\omega)$ model for $\text{YBa}_2\text{Cu}_3\text{O}_{6.95}$ at 10 K from Ref. 25. (d) Dispersion reported for $\text{YBa}_2\text{Cu}_3\text{O}_{6.85}$ at 11 K from Ref. 5.